

Research Article

Development and characterization of a functional smart PVA/NC/PCL nano-biocomposite using E. Coli Phage: Insights into physicochemical properties and antimicrobial activity

Malahat Safavi¹, Reza Rezaei Mokarram^{1*}, Mahmood Sowti Khiabani¹, Alireza Ostad Rahimi², Abolfazl Barzegar³

1. Department of Food Industry Science and Engineering, Faculty of Agriculture, University of Tabriz, Iran.

2. Nutrition Research Center, Department of Clinical Nutrition, School of Nutrition & Food Sciences, Tabriz University of Medical Sciences, Tabriz, Iran.

3. Research Institute for Fundamental Sciences (RIFS), University of Tabriz, Tabriz, Iran.

Abstract

Food packaging plays a critical role in preserving the freshness and quality of foods while preventing microbial spoilage. Advances in this field have led to the development of intelligent and active packaging systems incorporating nanotechnology. Among these innovations, electrospinning has gained attention for producing nanofibrous materials with high surface-to-volume ratios, enabling the efficient loading of active agents. In response to the growing concern over antibiotic-resistant bacteria, this study investigates the use of bacteriophages as an alternative antimicrobial agent. Lytic bacteriophages targeting *Escherichia coli* were isolated from Caspian seawater and immobilized onto electrospun nanofibers composed of polyvinyl alcohol (PVA), polycaprolactone (PCL), and bacterial nanocellulose (BNC). SEM confirmed successful phage immobilization, while TEM revealed their classification within the Siphoviridae and Podoviridae families. The addition of PCL to PVA enhanced the fibers' mechanical strength, reduced defects, and improved water resistance. Incorporating BNC further strengthened the nanofiber structure and enhanced its matrix properties. Antimicrobial testing using the disc diffusion method revealed an inhibition halo of 13 mm, exceeding that of the antibiotic ampicillin. Notably, the functionalized nanofibers retained antimicrobial efficacy for up to one month, with stable phage viability at 24°C, 4°C, and -20°C. These findings demonstrate the potential of electrospun nanofibers functionalized with bacteriophages as a sustainable solution for combating bacterial contamination in food packaging, enhancing food safety and extending shelf life.

KeyWords: Bacteriophages, Electrospinning, Polycaprolactone, Poly vinyl alcohol, Nanofiber, Bacterial Nanocellulose.

How to cite this article:

Safavi, M., Rezaei Mokarram, R., Sowti Khiabani, M., Ostad Rahimi, A., Barzegar, A., (2024). Development and characterization of a functional smart PVA/NC/PCL nano-biocomposite using E. Coli phage: Insights into physicochemical properties and antimicrobial activity. *Innov. Food Technol.*, 12 (1), 53-79. <https://doi.org/10.22104/ift.2025.7326.2193>

* Corresponding author: rmokarram@tabrizu.ac.ir



1. Introduction

Active packaging, a cutting-edge technology, integrates antimicrobials, antioxidants, and moisture-absorbing agents into polymeric materials, effectively extending the shelf life of perishable products. Within this realm, electrospun nanofibers have gained prominence for their high porosity, substantial surface-to-volume ratio, flexibility, and superior loading capacity, making them particularly suitable for active packaging (Nazari et al., 2019). Polyvinyl alcohol (PVA), selected for its synthetic, non-toxic, and water-soluble properties, exhibits robust thermal stability and excellent mechanical properties (Xiao et al., 2018).

The imperative exploration of alternative antibacterial treatments has arisen as a critical strategy to counter antibiotic overuse and effectively combat drug-resistant bacterial infections. In this context, the use of bacteriophages stands out as a leading antibacterial approach, among other options such as antibodies, probiotics, and antimicrobial peptides (Ghosh et al., 2019). Bacteriophages (phages), viruses that target and eliminate bacteria without harming human or animal cells, have demonstrated exceptional bactericidal efficacy in numerous research studies [4-6]. Recent advancements in bio-nanotechnology have further expanded the potential of phages as innovative functional nanomaterials, with applications in tissue regeneration and active food packaging (Shen et al., 2021).

The utilization of cellulose nanocrystals (CNC) as reinforcing materials enhances both the mechanical and thermal properties of nanofibers, contributing to improved nanofiber morphology and reduced diameters (Zhou et al., 2011). CNC-based nanofillers have demonstrated a remarkable ability to improve the mechanical and antibacterial properties of polymer matrices, such as PVA composites, making them

promising candidates for active packaging applications (Meng et al., 2023). These nanocrystals, with their nanometric dimensions, impressive strength, and biodegradability derived from renewable sources, facilitate the production of bio-based nanofibers with enhanced performance (Ribeiro et al., 2021).

In the pursuit of effective nanofiber fabrication, Polycaprolactone (PCL) emerges as a promising material due to its semi-crystalline hydrophobic nature and excellent hemo compatibility. However, despite its FDA-approved status, PCL electrospun membranes face challenges related to durability (Jiang et al., 2023).

A novel surface modification technique involving the predrying of PVA and electrospinning hydrophobic PCL nanofibers has proven to significantly enhance the physical and mechanical properties of the resulting PVA/PCL composites (Ahn et al., 2024). Addressing these challenges necessitates an advanced strategy—leveraging a combination of polymers in the electrospinning process to mitigate individual weaknesses and enhance overall nanofiber performance. The study focuses on *Escherichia coli* (*E. coli*), a gram-negative bacillus in the *Enterobacteriaceae* family responsible for various human infections (Doyle & Schoeni, 1987). *Escherichia coli* can be transmitted to humans through various pathways, with contaminated food being a major contributor [14, 15]. Ensuring the safety and quality of food products throughout the production, packaging, and distribution stages is essential. The rise of antibiotic-resistant bacteria further underscores the urgency of implementing effective preventive measures to combat food contamination. Incorporating controlled amounts of antimicrobial substances into packaging materials can extend the shelf life of food, aligning with consumer preferences for natural preservatives (Meshkani et al., 2013). Bacteriophages, harmless bacterial parasites,

emerge as a viable solution for controlling pathogenic bacteria throughout the food production process. However, challenges such as deactivation during food processing and the potential for bacterial resistance highlight the need for incorporating lytic phages into food packaging (Hagens & Loessner, 2010).

One approach involves immobilizing lytic phages on the surface of packaging material, facilitating their interaction with host cells on the food surface (Anany et al., 2011).

The primary objective of this study was to design and fabricate a two-layer nanofiber packaging system using electrospun materials based on PCL and PVA. PVA was chosen as the main component for its excellent mechanical properties, water solubility, and non-toxic nature, ensuring the safety of the packaging for food contact applications. This combination aimed to create a functional, safe, and effective packaging material for enhancing food preservation. Additionally, a layer of PCL was incorporated into the middle layer to further enhance the mechanical strength of the fibers. The results of this study not only deepen our understanding of electrospinning as a method for encapsulating bacteriophages but also pave the way for advancements in phage-based active food packaging technology, offering a promising solution for improving food safety and shelf life.

2. Materials and Methods

2.1. Materials

Escherichia coli (*E. coli* O157:H7) was obtained from the microbial collection of the Department of Microbiology and the Applied Pharmaceutical Research Center at Tabriz University of Medical Sciences. The specific lytic phage targeting *E. coli* was isolated from the coastal waters of the Caspian Sea using the method outlined by Liu et al. (Liu et al., 2006). Bacterial nanocellulose was synthesized using the method described by

Mahdieh Salari et al. [20]. Polyvinyl alcohol (PVA) with a hydrolysis degree of 87-89% and a molecular weight of 146-186 kDa, as well as polycaprolactone (PCL) with a molecular weight of 80,000, were sourced from Sigma-Aldrich. The SM buffer, consisting of 5/8 g NaCl, 2 g MgSO₄, 50 ml 1 M Tris-HCl, and 5 mL of a 2 wt% gelatin solution, was sourced from Merck, Germany. Nutrient Broth (NB), Muller Hinton Agar (MHA), and Luria Bertani (LB) culture media were obtained from Merck, Germany. All other chemicals and reagents utilized in the study were of analytical grade.

2.2. Methods

2.2.1. Preparation of Bacterial Nanocellulose

Bacterial nanocellulose pellicles were synthesized using "*Acetobacter xylinus*" in a molasses medium. For purification, the pellicles were washed with distilled water and treated with a 0.2 M NaOH aqueous solution at 90 °C for 30 min. The treated pellicles were then rinsed multiple times until neutralized. The purified BC pellicles were mechanically chopped into a cellulosic paste using a laboratory blender (Model 51BL32, Waring Co., USA) at 3500 rpm for 30 minutes.

To produce bacterial cellulose nanocrystals, the cellulosic paste was hydrolyzed with 98% sulfuric acid (50% w/w) at 50 °C for 40 minutes under vigorous stirring. The reaction was halted by diluting the suspension with approximately 10 times its volume of distilled water. The mixture was then centrifuged at 4000 g several times to concentrate the cellulose crystals and remove excess sulfuric acid. The sediment was collected and dialyzed against distilled water until a constant neutral pH was achieved.

Subsequently, mechanical treatment was performed through sonication in an ultrasonic bath (AS ONE, USD 4R, Japan) for 10 minutes at 40 kW while cooling in an ice bath. This was

followed by homogenization using a high-shear homogenizer (Heidolph Silent Crusher M, Germany) at 18000 rpm for 1 hour (Salari et al., 2018). The resulting aqueous suspension, containing approximately 0.8% (w/w) cellulose nanocrystals, was stored in a refrigerator at 4 °C for future use.

2.2.2. Preparing Electrospinning Solutions

The electrospinning solutions were meticulously prepared in two distinct steps. Initially, 10 g of PVA powder was dissolved in 100 mL of preheated water and vigorously mixed for 4 hours to ensure complete dissolution. Subsequently, 2.5, 5, and 7.5 g of BNC powder was meticulously added to the solution, creating a homogeneous mixture.

In the second step, a solution for electrospinning was prepared by dissolving 15 g of PCL powder in 100 ml of dichloromethane solvent. The solution was meticulously mixed for 30 min to achieve the desired consistency and homogeneity.

2.2.3. Bacterial Strain Preparation and Specific Lytic Phage Activation

The bacteriophage strain originated from the coastal waters of the Caspian Sea. Seawater samples was filtered through 0.22-micrometer pore-size membranes, and the presence of phages was assessed using the two-layer agar method to detect plaque formation (Liu et al., 2006). Lyophilized *Escherichia coli* bacteria were aseptically reconstituted in a laminar flow hood, breaking the vial under sterile conditions. A 0.5 mL aliquot of sterile Nutrient Broth (NB) was then added using a micropipette to prepare a bacterial suspension. This suspension was subsequently transferred onto Luria-Bertani (LB) solid culture medium and adjusted to a 0.5 McFarland standard before incubation at 37°C for 24 hours (Ranjbar et al., 2014). The LB culture medium was initially enriched with

calcium chloride to activate the specific phage. Phage multiplication was facilitated using the double-layer agar method, and the positive plates were stored at 4°C for preservation (Anany et al., 2011).

2.2.4. Electrospinning Process

The electrospinning process was conducted utilizing the ES1000 model electrospinning machine, manufactured by Fannavar nanomeghyas Company in Iran. Equipped with a drum collector, this advanced system enabled the precise fabrication of nanofiber mats. The process was carried out for 30 minutes under controlled conditions, including a 16 cm working distance, a drum speed of 200 RPM, a nozzle angle of 90°, a flow rate of 2 mL/hr, and a high-voltage supply of 24 kV. The electrospinning process was performed using a dual-nozzle setup, with one nozzle dedicated to electrospinning PCL and the other delivering a composite solution of PVA, BNC, and phages. Both nozzles were fitted with stainless-steel No. 18 blunt-ended needles to ensure precise and controlled solution delivery. The dual-nozzle configuration allowed for the simultaneous deposition of distinct materials, facilitating the fabrication of hybrid nanofibrous structures. Under optimized conditions, this approach ensured the successful production of nanofiber mats with uniform morphology and tailored properties, making them suitable for effective active packaging applications.

2.2.5. Immobilization of Phage on Electrospun Fibers within a PCL/PVA/BNC

To immobilize the phage, electrospinning was employed by incorporating a bacteriophage suspension into a polymeric solution. Specifically, 5 mL of a phage solution (approximately 10¹⁰ PFU/mL) was added to the PVA solution containing varying concentrations of BNC. The resulting suspension was

electrospun under optimal conditions, and the formed nanofibers were left at room temperature for 24 hours to stabilize (Goddard & Hotchkiss, 2007).

2.2.6. Scanning Electron Microscope Imaging to Verification Nanocellulose Matrix

Phage immobilization on the electrospun fibers was verified using scanning electron microscopy (SEM) with a MIRA3 FEG-SEM (Tescan, Czech Republic). Before imaging, the fibers were coated with a gold layer for 5 minutes to enhance conductivity. Image analysis was conducted under a 26 kV acceleration voltage (Tolba et al., 2010).

2.2.7. Morphological Examination of Bacteriophages using Transmission Electron Microscopy (TEM)

For the morphological analysis of bacteriophages, 10 μ L of the bacteriophage suspension was deposited onto a carbon-coated

Equation. 1

$$\text{Moisture Absorbance Rate} = \frac{\text{Final Weight} - \text{Initial Weight}}{\text{Initial Weight}} \times 100$$

For the determination of water content, 2 \times 2 cm fiber samples were placed in a desiccator at 55% relative humidity overnight, then weighed. The samples were subsequently dried in an oven at 105°C for 6 hours, cooled in the desiccator, and

Equation. 2

$$\text{Water Content (\%)} = \frac{\text{Initial Weight} - \text{Final Weight}}{\text{Initial Weight}} \times 100$$

For assessing water solubility, 100 mg of each fiber, previously dried in an oven at 105°C, was immersed in 50 mL of water and agitated for 6 hours at room temperature. After incubation, the

Equation. 3

$$\text{Solubility Rate (\%)} = \frac{\text{Weight of Insoluble Residue}}{\text{Initial Weight}} \times 100$$

grid and allowed to dry at room temperature. Negative staining was then performed using a 2% uranyl acetate solution. The stained grids were examined using a transmission electron microscope (LE0906: Zeiss, Germany), and images of the targeted areas were captured using a Gatan Multiscan 791 CCD camera.

2.2.8. Water Absorption, Water Content, Water Solubility and Water Contact Angle Measurements

To assess the water absorption capacity of the optimized fabricated fibers, 2 \times 2 cm fiber samples were initially weighed and placed in a desiccator with 0% humidity, achieved using calcium sulfate, for dehydration. The fibers were then transferred to a desiccator maintained at 55% relative humidity using a saturated calcium nitrate solution, where they remained until reaching equilibrium weight. The moisture absorbance rate was calculated using the equation 1:

weighed again. The water content was calculated based on the difference in weight before and after drying. The water content was then calculated using the equation 2:

fiber solution was filtered, and the insoluble residue was dried in an oven at 105°C before weighing. The solubility rate was determined using the equation 3:

The dynamic water contact angle was employed to gain deeper insights into the water absorption behavior of the mats. This measurement was conducted using a G10 device from KRUSS, Germany, renowned for its precision and reliability in assessing surface interactions with liquids.

2.2.9. Fourier Transform Infrared Spectroscopy (FTIR):

To elucidate the chemical structure and interactions among the components, Fourier Transform Infrared (FTIR) spectroscopy was conducted over the range of 4000–400 cm^{-1} (Tensor 27, Bruker, Germany). FTIR spectra were acquired with a resolution of 4 cm^{-1} and an average of 256 scans per spectrum. All measurements were performed at room temperature and reported based on transmission. An empty KBr disc served as the reference, and its spectrum was subtracted from the sample spectrum to eliminate any spectral artifacts arising from KBr impurities and water (Mahoutforoush et al., 2023).

2.2.10. X-ray Diffraction (XRD) Analysis:

X-ray diffraction (XRD) analysis of films was conducted using a Bruker D5000 instrument (Siemens, Germany) equipped with $\text{CuK}\alpha$ radiation (wavelength = 0.154 nm). The system was operated at 40 kV and 30 mA. Measurements were performed at room temperature over a 2θ range of 5° to 50°, with a step size of 0.05° and a scanning speed of 1° per minute (Salari et al., 2018).

2.2.11. Thermal Analysis:

The thermal properties of the films were assessed using Differential Scanning Calorimetry (DSC) (F3 200 DSC, Netzsch, Germany). Film samples were cut into small pieces and placed on a sample pan, with an

empty pan used as the reference. The melting point (T_m) of the films was determined through heating scans performed at a rate of 10°C/min, ranging from 30°C to 250°C, under a constant flow of nitrogen gas (Salari et al., 2018).

2.2.12. Mechanical Properties Analysis

The mechanical properties of the films, including Ultimate Tensile Strength (UTS), Young's Modulus (YM), and Strain to Break (SB), were evaluated according to the ASTM D882-91 standard (ASTM, 1996). Prior to testing, the samples were conditioned for 24 hours at a relative humidity of 57%. Each film was then precisely cut into a dumbbell shape (8 cm × 0.5 cm) and securely positioned between the grips of the testing machine. The primary grip breaking length and crosshead speed were carefully set to 50 mm and 5 mm/min, respectively, to ensure consistent and accurate measurements (Salari et al., 2018).

2.2.13. Evaluation of Antimicrobial Activity, Phage Plaque Observation, and Titer Determination

Half McFarland's concentration of *E.coli* bacteria were cultured in an LB liquid medium at 37°C for 24 hours. Afterward, 100 μL of the host bacteria were mixed with 5 mL of semi-solid LB medium and then spread onto an LB agar plate. Following a 15-minute stabilization period, a serial dilution of the phage was prepared. Then, 10 μL of the diluted phage solution was carefully added to the surface of the actively growing bacterial culture, ensuring uniform distribution across the plate. The plates were incubated overnight at 37°C. The appearance of plaques the following day indicated the phage's ability to lyse the host bacteria. The concentration of phage particles in the suspension was quantified by counting the plaques and using the following equation 4:

Equation 4: Determination of Phage Number (PFU/mL) = $\left(\frac{\text{Number of plaques}}{\text{Dilution factor}}\right) \times \text{Volume of phage solution plated (mL)}$ (Vonasek et al., 2014).

2.2.14. Assessment of the Antimicrobial Activity of Nano BioComposite

The antimicrobial activity of the electrospun active nanofibers was evaluated using the disk diffusion method. Discs (6 mm in diameter) were prepared from electrospun PCL/PVA/BNC/bacteriophage fibers and placed onto a Muller Hinton Agar (MHA) plate pre-inoculated with an *Escherichia coli* suspension at a concentration of 10^{10} CFU/mL. Nanofibers without the phage served as the negative control, while a disc containing ampicillin was selected as the positive control. Subsequently, the plates were incubated at 37°C for 24 hours, after which the antimicrobial activity was assessed by measuring the diameter of the inhibition zone (Topuz et al., 2021).

2.2.15. Assessment of the Antimicrobial Efficacy of Immobilized Phages Over Time

To evaluate the long-term antimicrobial efficacy of phages immobilized on electrospun fibers, the active nanofibers were stored in an airtight container at room temperature (25°C) for one month. Saturated barium chloride was used to maintain a relative humidity of 80–86% throughout the storage period. The host bacterium underwent incubation at 37°C for 24 hours. Subsequently, a bacterial suspension was prepared with a dilution of 10^3 CFU/mL. Circular slices (2 cm in diameter) were extracted from both active and control nanofibers and immersed in 9 mL of the bacterial suspension. Bacterial counts in the suspension were measured at seven time points—days 1, 5, 10, 15, 20, 25, and 30—following the storage of active and control nanofibers.

2.2.16. Statistical analysis

All experiments in this study were conducted in triplicate. Statistical analysis was performed

using one-way and two-way analysis of variance (ANOVA), followed by multiple comparisons using the Tukey honest significant difference (HSD) test. Data analysis was carried out using GraphPad Prism (version 9, San Diego, CA), with a significance threshold set at $P < 0.05$.

3. Results and Discussion

3.1. Physical properties

3.1.1. Moisture Content, Water Solubility, and Water Absorption

Fig 1 presents a comparative analysis of the moisture content, water solubility, and water absorption characteristics for PVA, PCL, PVA-PCL, and PVA-PCL with varying concentrations of nanocellulose (NC). The results highlight significant differences in these properties influenced by the material composition and the inclusion of NC. As shown in Fig 1a, moisture content increases significantly with the incorporation of NC into the PVA-PCL matrix. Among the samples, PVA exhibits the highest moisture content, reflecting its strong hydrophilic nature. The incorporation of NC into the PVA-PCL matrix at increasing concentrations (2.5%, 5%, and 7.5%) further elevates moisture content, with PVA-PCL-NC (7.5%) displaying the highest values. This trend suggests that NC, owing to its hydrophilic properties, enhances the water-attracting capability of the composite. Similar patterns of hydrophilic reinforcement by NC have been observed in other polymer matrices (Jamróz et al., 2019). PCL, a hydrophobic polymer, shows the lowest moisture content, demonstrating its inherent resistance to water uptake (Zheng et al., 2021). The data in Fig 1.b reveal a decreasing trend in water solubility as NC concentration increases in PVA-PCL composites. PVA alone



exhibits the highest solubility, while PCL demonstrates minimal solubility due to its hydrophobic nature. The PVA-PCL combination shows intermediate solubility, which progressively decreases with the incorporation of NC. This decrease suggests that NC enhances the crystalline structure and crosslinking density of the composite, reducing its solubility in water (Singhaboot et al., 2023). The results in Fig 1.c show that the incorporation of NC significantly increases water absorption in PVA-PCL composites. While PVA-PCL alone exhibits low water absorption, the addition of NC at increasing concentrations (2.5%, 5%, and 7.5%) systematically increases the absorption capacity. This effect is likely due to NC's ability to reinforce the polymer matrix, increasing its hydrophilicity properties that boost water penetration. As expected, PCL exhibits minimal water absorption, consistent with its hydrophobic properties (Zhao et al., 2020).

The results demonstrate the impact of NC on the moisture-related properties of the PVA-PCL matrix. Adding NC increases the overall moisture content and absorption due to its hydrophilic nature while reducing water solubility by reinforcing the matrix structure. This dual effect highlights NC's role as both a hydrophilic agent and a structural reinforcer (Jamróz et al., 2019).

At higher NC concentrations, the enhanced crystallinity and barrier properties of the composite materials are particularly notable. These improvements could be advantageous in applications where controlled water interaction and stability are critical, such as in biomedical scaffolds or food packaging (Singhaboot et al., 2023). Future studies could explore the effect of NC particle size and surface modifications on these properties for further optimization (Zhao et al., 2020).

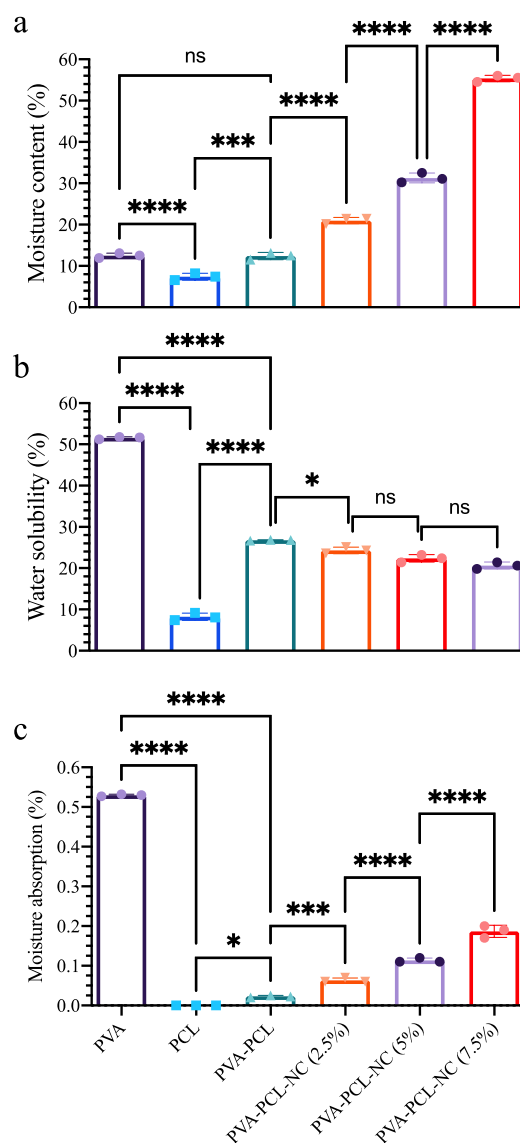


Fig 1. a. Moisture Content, b. Water Solubility, and c. Water Absorption of Nanofibers. Poly vinyl alcohol nanofibers (PVA), Polycaprolactone nanofibers (PCL), Poly vinyl alcohol + Polycaprolactone nanofibers (PVA-PCL), and Poly vinyl alcohol + Polycaprolactone + nanocellulose nanofibers (PVA-PCL-NC). The data, mean \pm SD (n = 3). NS: not significant, **p < 0.01, ****p < 0.0001, versus multiple comparisons.

3.1.2. Surface hydrophobicity

As shown in Fig 2, the surface hydrophobicity of the electrospun nanofibers was evaluated using contact angle measurements. This parameter provides critical insight into the wettability of the biocomposite surfaces, which directly affects their functionality in applications such as antimicrobial activity and biocompatibility.

The contact angle for PVA nanofibers was the lowest (46°), indicating a highly hydrophilic surface. This is attributed to the hydroxyl groups in the PVA structure, which promote water attraction. In contrast, PCL nanofibers exhibited the highest contact angle (140°), confirming their hydrophobic nature due to the absence of



polar functional groups in their aliphatic polyester backbone.

The PVA-PCL blend nanofibers exhibited an intermediate contact angle of 133° , indicating that blending PVA and PCL moderates the extreme hydrophilic and hydrophobic characteristics of the individual polymers. The incorporation of bacterial cellulose (BC) and increasing concentrations of nanocellulose (NC) into the PVA-PCL matrix progressively reduced the contact angle. The contact angle values for PVA-PCL-NC composites were 104° for 2.5% NC, 78° for 5% NC, and 55° for 7.5% NC, reflecting a significant increase in surface hydrophilicity with higher NC content.

The progressive reduction in contact angle with increasing NC concentration can be attributed to the hydrophilic nature of NC, which introduces additional hydroxyl groups to the composite surface, enhancing water-attracting properties. This trend is consistent with prior studies where

NC was shown to modulate surface hydrophilicity in polymeric composites (Panchal et al., 2019). Furthermore, the enhanced hydrophilicity of the bio-composites is beneficial for biomedical applications, as it facilitates improved cell adhesion and biocompatibility (Zhao et al., 2020).

The moderate hydrophobicity observed for the PVA-PCL blend without NC suggests its potential for applications where controlled water interaction is needed, such as water-resistant packaging. In contrast, the significant hydrophilicity achieved with PVA-PCL-NC (7.5%) makes it highly suitable for biomedical applications that require strong interaction with aqueous environments, such as wound dressings and antimicrobial scaffolds. The tunable nature of the surface properties underscores the versatility of these bio-composites, making them adaptable for a wide range of applications.

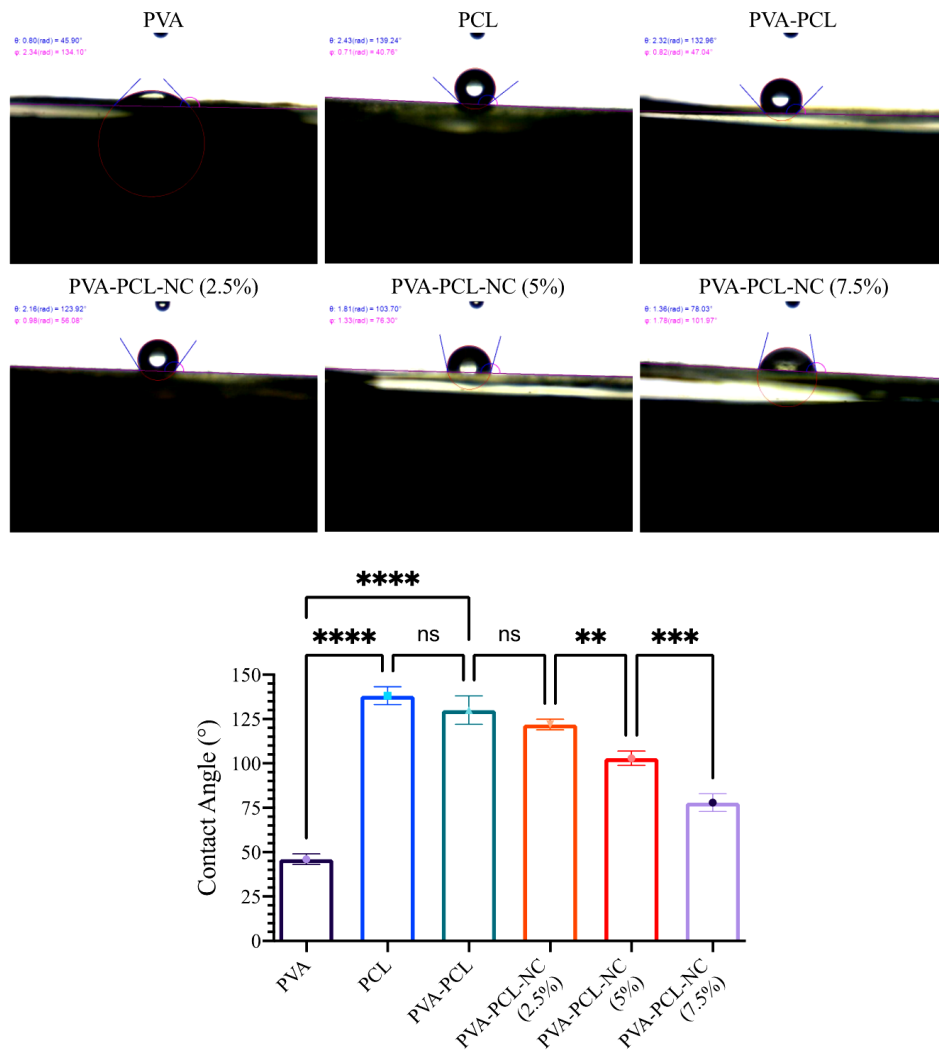


Fig 2. Contact angle measurements of PVA, PCL, PVA-PCL, and PVA-PCL-NC composites with varying concentrations of nanocellulose (2.5%, 5%, and 7.5%). Data are presented as mean \pm SD (n = 3). Statistical significance: ns: not significant, **p < 0.01, ***p < 0.0001.

3.2. Mechanical properties

Fig 3 illustrates the ultimate tensile strength (UTS) and strain to break (SB) for various nanofibers, including PVA, PCL, PVA-PCL blends, and PVA-PCL-NC composites with increasing concentrations of nanocellulose (NC). These parameters provide insights into how the mechanical performance of the materials is influenced by their composition and the incorporation of NC.

The results show distinct variations in UTS across the tested groups. PVA exhibited a moderate UTS of 0.31 MPa, attributed to its inherent mechanical properties and the hydrogen bonding between polymer chains. In contrast, PCL had the lowest UTS (0.16 MPa), reflecting its flexible and less rigid nature. The PVA-PCL blend demonstrated a slightly higher UTS (0.23 MPa) than PCL, but lower than pure PVA, indicating partial reinforcement from the blend, though the weaker

mechanical properties of PCL contributed to reduced overall performance.

The incorporation of NC significantly enhanced UTS in the PVA-PCL-NC composites. The UTS increased progressively with higher NC content, reaching 0.33 MPa at 2.5% NC, 0.39 MPa at 5% NC, and 0.45 MPa at 7.5% NC. This improvement can be attributed to NC's high stiffness and strength, which acts as a reinforcing agent by effectively transferring stress and improving the load-bearing capacity of the nanofiber matrix. Similar trends have been reported in other studies, where NC addition improves the mechanical performance of polymer composites (Ejara et al., 2021).

For SB, PVA, PCL, and PVA-PCL exhibited similar strain values, reflecting limited elongation capability due to the inherent brittleness of PVA and the less elastic nature of the blend. However, the addition of NC significantly improved the SB of the nanofibers. At 2.5% NC, the SB increased substantially compared to PVA, PCL, and PVA-PCL fibers. Further increases in NC concentration (5% and 7.5%) maintained high SB values,

highlighting the role of NC in enhancing flexibility by creating a robust yet elastic network within the matrix.

This increase in SB is likely due to the uniform dispersion of NC within the polymer matrix at lower concentrations, facilitating effective load distribution and preventing premature failure. However, at higher NC content (7.5%), SB remained stable, possibly due to the onset of agglomeration, which slightly reduces matrix mobility. These findings align with prior research, where CNC-enhanced polymer composites demonstrated improved tensile properties without significant trade-offs in elongation (Meng et al., 2024).

The mechanical properties of the nanofibers were significantly improved with the addition of NC, as evidenced by increased UTS and SB. These findings demonstrate the potential of PVA-PCL-NC composites for applications requiring enhanced strength and flexibility, such as tissue engineering scaffolds or antimicrobial membranes. Further optimization of NC concentration and dispersion can maximize mechanical performance.

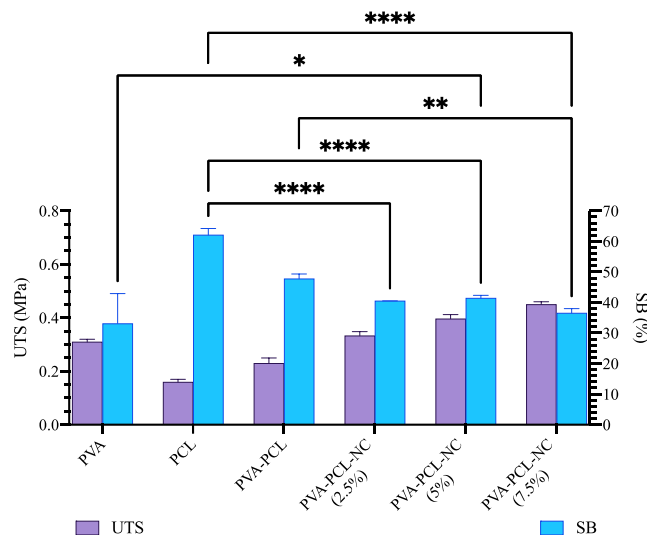


Fig 3. Tensile properties of Polyvinyl alcohol (PVA), Polycaprolactone (PCL), PVA-PCL blends, and PVA-PCL nanocomposites with 2.5%, 5%, and 7.5% NC. Data represent mean \pm SD ($n = 3$). Statistical significance: $p < 0.01$; ns = not significant.

3.3. FTIR

The Fourier Transform Infrared (FT-IR) spectra of pure polyvinyl alcohol (PVA), polycaprolactone (PCL), their blend (PVA-PCL), and nanocomposites with nanocellulose (PVA-PCL-NC at 5% and 7.5% NC content) are illustrated in Fig 4. The FT-IR analysis was conducted to investigate the chemical interactions and compatibility between the components of the nanocomposite system.

In the spectrum of pure PVA, characteristic absorption bands were observed at approximately 3300 cm^{-1} , corresponding to the O–H stretching vibrations, indicating the presence of hydroxyl groups. The peaks at approximately 2940 cm^{-1} and 2900 cm^{-1} can be attributed to the asymmetric and symmetric stretching vibrations of C–H bonds. Additionally, the sharp band at around 1700 cm^{-1} is indicative of C=O stretching, likely arising from residual hydrolyzed acetate groups. The bands around 1100 cm^{-1} represent C–O stretching vibrations, further confirming the structure of PVA.

For the PCL spectrum, the characteristic peaks include the prominent absorption band at $\sim 1720\text{ cm}^{-1}$, corresponding to the stretching vibrations of the carbonyl (C=O) groups. The peaks at $\sim 2930\text{ cm}^{-1}$ and $\sim 2860\text{ cm}^{-1}$ represent asymmetric and symmetric C–H stretching vibrations of the aliphatic chain. The bands observed at $\sim 1170\text{ cm}^{-1}$ and $\sim 1295\text{ cm}^{-1}$ correspond to C–O–C stretching vibrations, typical of ester groups in PCL.

The FT-IR spectrum of the PVA-PCL blends exhibits absorption bands characteristic of both PVA and PCL, indicating the successful blending of the two polymers. The O–H stretching peak from PVA ($\sim 3300\text{ cm}^{-1}$) slightly broadens, suggesting potential intermolecular hydrogen bonding between the hydroxyl groups of PVA and the carbonyl groups of PCL. The C=O stretching band at $\sim 1720\text{ cm}^{-1}$ from PCL remains prominent, confirming the presence of the PCL component in the blend.

Several notable changes were observed in the FT-IR spectra for the nanocomposites containing nanocellulose (PVA-PCL-NC 5% and 7.5%). In both cases, the O–H stretching band ($\sim 3300\text{ cm}^{-1}$) becomes broader and shifts slightly, indicating enhanced hydrogen bonding interactions between the nanocellulose, PVA, and PCL. The intensity of the C=O stretching band ($\sim 1720\text{ cm}^{-1}$) increases with the addition of nanocellulose, suggesting the incorporation of nanocellulose into the polymer matrix and interaction with the carbonyl groups of PCL.

Additionally, the presence of nanocellulose is confirmed by the enhanced absorption bands in the fingerprint region. The peaks corresponding to C–O stretching vibrations ($\sim 1100\text{ cm}^{-1}$) show increased intensity in the PVA-PCL-NC spectrum compared to the pure polymers and the blend. This enhancement signifies the successful incorporation of nanocellulose, which is rich in hydroxyl groups, into the composite matrix.

Interestingly, at higher nanocellulose content (7.5%), the FT-IR spectrum shows a further increase in intensity and broadening of the O–H and C=O bands, highlighting stronger intermolecular interactions. The increased intensity of the bands in the fingerprint region further confirms the reinforcing effect of nanocellulose within the polymer matrix.

In summary, the FT-IR analysis demonstrates the compatibility and interaction between PVA, PCL, and nanocellulose in the nanocomposite fibers. Incorporating nanocellulose enhances hydrogen bonding and reinforces the composite structure, which is critical for improving functional and antimicrobial properties of the PVA/BC/PCL nano-bio composite.

The implemented spectroscopic analytical approaches allowed for the chemical identification and visualization of the electrospun fiber mats. FT-IR spectroscopy, used for chemical analysis, confirmed the presence of unaltered polymer fibers,

displaying characteristic PVA-PCL bands consistent with the reference spectra of PVA and PCL (Zidan et al., 2019).

The FT-IR results revealed enhanced hydrogen bonding with the incorporation of nanocellulose (NC), especially at higher NC content (7.5%), as evidenced by the broadening and intensification of the O–H and C=O stretching bands. These changes confirm strong intermolecular interactions between PVA, PCL, and NC, contributing to the improved functional properties observed in PVA-PCL-NC composites. Comparatively, our findings align with previous studies, such as those by Ji Xinbin et al. (2021), which reported similar hydrogen bonding effects in PVA composites reinforced with cellulose nanocrystals. These interactions play a crucial role

in determining the chemical compatibility and stability of nanocomposite systems (Ji et al., 2021).

Following the chemical analysis of the electrospun fiber mats, their mechanical properties were evaluated. The mechanical performance of these fiber networks is influenced by multiple factors, including fiber diameter, network architecture, and polymer composition. Additionally, variations in collector rotation speed can induce oriented fiber deposition, further affecting the mechanical properties. Hence, uniaxial tensile testing was conducted both parallel and perpendicular to the rotation direction of the collector to evaluate mechanical properties in both directions and detect any anisotropy resulting from fiber alignment (Chen et al., 2009).

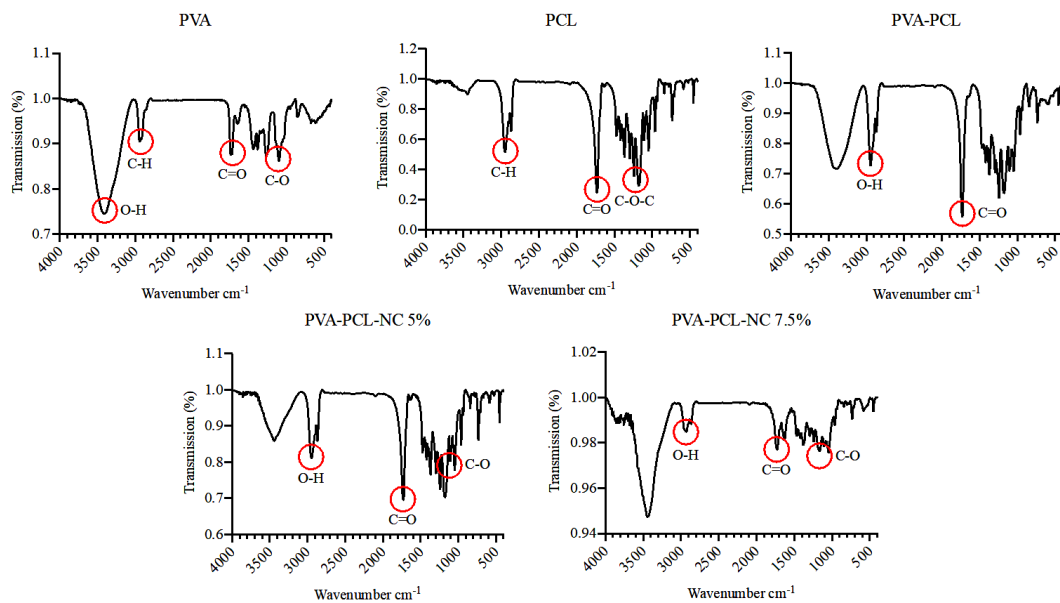


Fig 4. represents the FT-IR spectrum of PVA) Poly vinyl alcohol nanofibers, PCL) Polycaprolactone nanofibers, PVA-PCL) Poly vinyl alcohol + Polycaprolactone nanofibers, and PVA-PCL-NC) Poly vinyl alcohol + Polycaprolactone + nanocellulose nanofibers (at different percentages).

3.4. XRD

The X-ray diffraction (XRD) patterns of PVA, PCL, PVA-PCL, and PVA-PCL-NC nanofibers with varying concentrations of nanocellulose (NC) (2.5%, 5%, and 7.5%) are presented in Fig

5. These results provide insights into the crystalline structures and interactions within the composite materials.

The XRD pattern of PVA nanofibers exhibited a broad diffraction peak around $2\theta = 19.5^\circ$, confirming its semicrystalline nature. This peak

originates from interchain hydrogen bonding in PVA, which facilitates the formation of small crystalline domains embedded within an amorphous matrix. These results are consistent with previous studies that have reported the semicrystallinity of electrospun PVA fibers (Bhardwaj & Kundu, 2010).

In contrast, PCL nanofibers exhibited sharp and well-defined peaks at $2\theta = 21.3^\circ$ and 23.6° , corresponding to the (110) and (200) crystalline planes of PCL, respectively. These peaks highlight the highly crystalline nature of PCL, consistent with the regular packing of its polymer chains. Similar crystalline peaks have been observed in electrospun PCL nanofibers, further confirming their semicrystalline structure (Zhou et al., 2006).

The XRD pattern of PVA-PCL nanofibers exhibited characteristic peaks of both PVA (broad peak at 19.5°) and PCL (sharp peaks at 21.3° and 23.6°). However, a slight reduction in the intensity of the PCL peaks was observed, suggesting partial disruption of PCL's crystalline domains due to interactions with PVA. This disruption may result from intermolecular interactions, such as hydrogen bonding or van der Waals forces, forming a more homogenous composite with intermediate crystalline behavior. Similar reductions in crystallinity have been reported in PVA-PCL blends due to polymer chain interactions (Azari et al., 2022). The incorporation of nanocellulose into the PVA-PCL matrix altered the XRD patterns significantly.

At a 2.5% NC concentration, the intensity of the PVA peak at 19.5° slightly increased, suggesting that NC promotes hydrogen bonding and reinforces the crystalline regions of PVA. The PCL peaks remained present but showed a slight decrease in intensity, indicating minor disruption of PCL crystallinity. This observation aligns with previous studies showing that nanocellulose can act as a reinforcing filler in polymer matrices,

enhancing crystalline regions while preserving structural integrity (Dufresne, 2013).

At a 5% NC concentration, a further reduction in PCL peak intensity was observed, along with broadening of the PVA peak. This trend suggests that increasing NC content disrupts the regular packing of both PVA and PCL chains, resulting in a more amorphous composite. The enhanced amorphous nature can be attributed to the improved dispersion of NC, which interacts with polymer chains and disrupts crystallinity.

At a 7.5% NC concentration, a weak new peak emerged around $2\theta = 22.5^\circ$, corresponding to the crystalline structure of nanocellulose. This confirms the successful incorporation of NC into the polymer matrix and its influence on the composite's crystalline behavior. The broadening of peaks at this concentration suggests that NC further disrupts polymer chain packing, enhancing uniformity while slightly reducing overall crystallinity. These findings are consistent with previous studies, which have reported that high NC concentrations reduce crystallinity due to strong nanofiller-polymer interactions (Cho & Park, 2011).

The observed decrease in crystallinity with increasing NC content aligns with findings from other researchers. Studies have demonstrated that NC incorporation in PVA or PCL matrices disrupts polymer chain packing, increases amorphous regions, and simultaneously reinforces the matrix mechanically (Palali, 2019). Moreover, the appearance of a nanocellulose crystalline peak at 22.5° highlights its successful integration into the composite, supporting prior research that shows NC maintains its crystallinity even at higher loadings within the matrix (Moon et al., 2011).

The XRD analysis revealed that the incorporation of NC into PVA-PCL nanofibers altered their crystalline properties, with higher NC concentrations leading to a reduction in

crystallinity and an enhancement of amorphous regions. This structural modification underscores the potential of nanocellulose as a reinforcing agent in composite materials,

offering a balance between improved dispersion and mechanical properties, while reducing crystallinity.

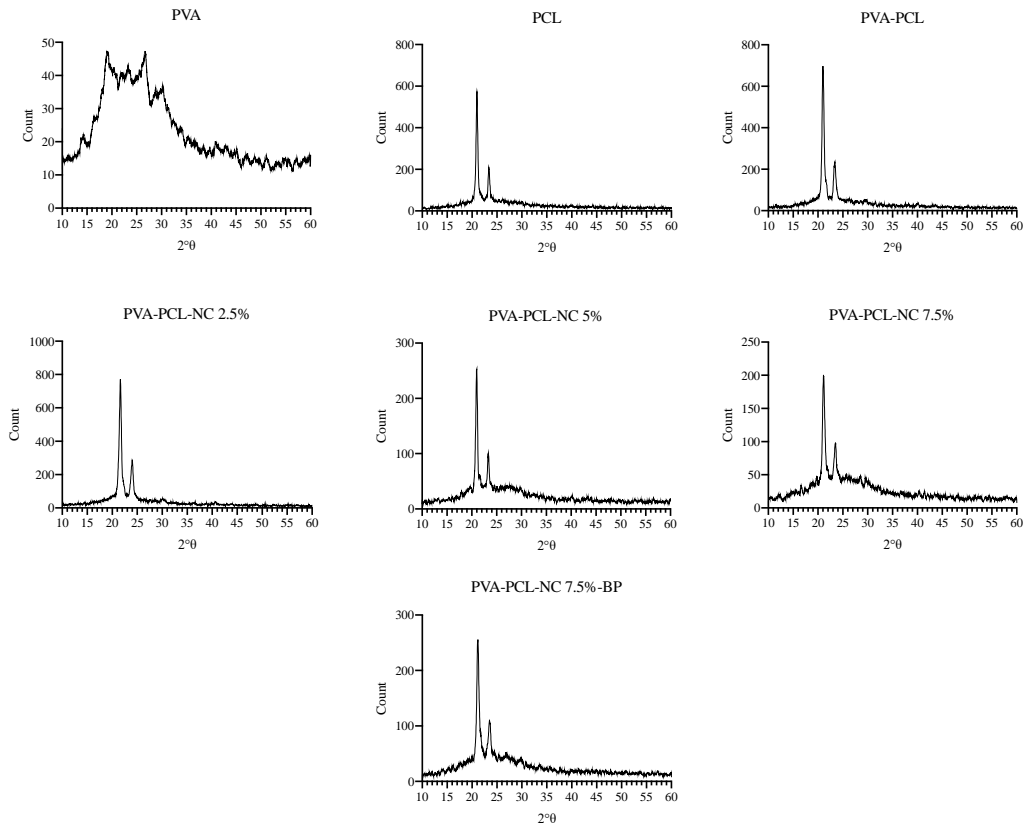


Fig 5. X-ray diffraction (XRD) analysis of Polyvinyl alcohol nanofibers (PVA), Polycaprolactone nanofibers (PCL), Polyvinyl alcohol + Polycaprolactone nanofibers (PVA-PCL), and Polyvinyl alcohol + Polycaprolactone + nanocellulose nanofibers at different percentages (PVA-PCL-NC).

3.5. Thermal properties

In Fig 6, the thermal properties of the prepared nanocomposite fibers—pure PVA, pure PCL, their blend (PVA-PCL), and PVA-PCL with varying nanocellulose (NC) concentrations (2.5%, 5%, and 7.5%)—were analyzed using differential scanning calorimetry (DSC) and thermogravimetric analysis (TGA). The results obtained are summarized below and compared with related studies in the field.

The DSC thermogram of pure PVA nanofibers showed a characteristic melting temperature (T_m) around 200°C, corresponding to its crystalline

structure. Meanwhile, the TGA analysis indicated a two-stage decomposition process (Rasheed et al., 2024). The first stage of the TGA analysis involved moisture evaporation at lower temperatures, while the second stage reflected the breakdown of the polymer backbone. Similarly, PCL nanofibers exhibited a melting temperature around 60°C, consistent with its semicrystalline nature, and a single degradation peak at higher temperatures, indicating its relatively higher thermal stability compared to PVA. These results are in agreement with prior studies that report similar thermal profiles for pure PVA and PCL polymers (Rasheed et al., 2024).



Thermal Properties of PVA-PCL Blend Nanofibers

The PVA-PCL blend nanofibers exhibited combined thermal characteristics of both PVA and PCL, with distinct melting points for each polymer. This dual behavior suggests a successful blending of the two polymers. The degradation onset temperature of the blend shifted to a higher temperature compared to the individual polymers, indicating improved thermal stability, likely due to enhanced intermolecular interactions between the polymer chains. Similar findings were reported by Zhang et al. (2019), who observed improved thermal stability in PVA-PCL blends as a result of synergistic interactions between the two polymers (Huang et al., 2019).

The addition of nanocellulose (NC) to the PVA-PCL matrix resulted in significant changes to the thermal properties. At a 7.5% NC concentration, the TGA results showed a higher degradation onset temperature compared to the neat PVA-PCL blend, confirming that nanocellulose acts as a reinforcing agent. The enhancement in thermal stability is attributed to the high thermal stability of NC, which restricts polymer chain mobility and delays decomposition. This observation aligns with the findings of Li et al. (2020), who reported similar improvements in thermal stability upon incorporating nanocellulose into polymer matrices (Li et al., 2020).

DSC results revealed a slight shift in melting temperatures and a reduction in the intensity of melting peaks with increasing NC content. This suggests a decrease in crystallinity due to the disruption of the polymer's regular chain alignment by NC, leading to a more amorphous structure. A similar reduction in crystallinity upon the addition of NC has been documented in other studies on nanocellulose-reinforced composites (Khoo et al., 2016).

The observed improvements in thermal stability and the reduction in crystallinity in PVA-PCL-NC composites are consistent with the behavior of other polymer-nanocellulose systems. For instance, in PLA-based nanocellulose composites, researchers reported increased thermal stability and disrupted crystalline phases due to strong polymer-NC interactions. These findings suggest that the incorporation of NC into PVA-PCL blends not only enhances thermal performance but also alters the crystalline structure, potentially broadening their applications in areas requiring enhanced thermal resistance.

The thermal analysis of PVA-PCL nanocomposite fibers with nanocellulose revealed a marked enhancement in thermal stability and modifications to the crystalline structure. At higher NC concentrations (7.5%), the composites exhibited optimal thermal properties, attributed to the reinforcing effects of nanocellulose.

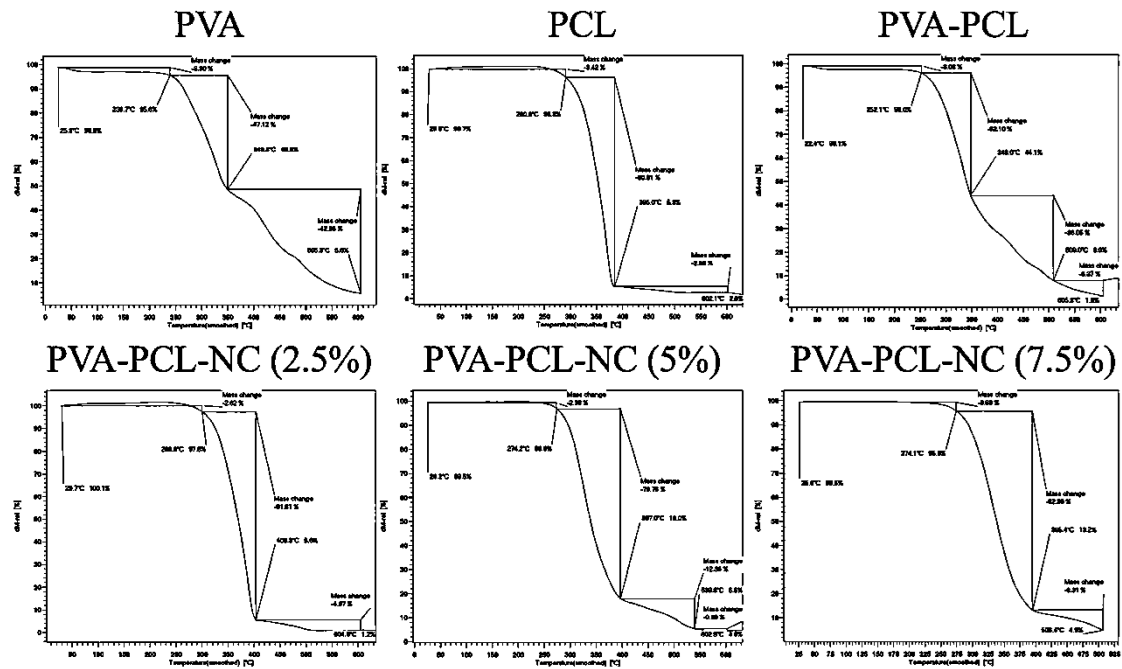


Fig 6. Thermal properties of Poly vinyl alcohol nanofibers (PVA), Polycaprolactone nanofibers (PCL), Poly vinyl alcohol + Polycaprolactone nanofibers (PVA-PCL), and Poly vinyl alcohol + Polycaprolactone + nanocellulose nanofibers at different percentages (PVA-PCL-NC).

3.6. Microstructure

SEM images of the fabricated nanofibers are presented in Fig. 7, showcasing a diverse range of compositions and structures. Fig 7.a depicts pure PVA nanofibers, revealing a network of ultrafine fibers with random orientations. These fibers exhibit consistent diameters throughout the image, contributing to their uniform appearance.

In Fig. 7.b, PCL nanofibers share similarities with PVA nanofibers but display slightly thicker fibers with a smoother, more uniform texture. The electrospinning of PVA blended with PCL (Fig. 7c) results in fibers that exhibit characteristics of both polymers, displaying a range of diameters and variations in surface smoothness.

The introduction of nanocellulose (NC) into the PVA-PCL nanofibers, as shown in Fig. 7d, results in rougher, more textured areas, indicating the successful incorporation of NC into the nanofiber matrix. This modification alters the surface

morphology, suggesting potential improvements in properties such as mechanical strength and biocompatibility.

Fig 7.e demonstrates the successful immobilization of bacteriophages onto the nanofiber matrix. The presence of bacteriophages within the nanofibers is evident. Antimicrobial active food packaging demands stability of the bioactive cargo over prolonged storage periods while ensuring controlled and consistent release. Moreover, fiber packaging necessitates robust mechanical properties for practical application. Scanning electron microscopy (SEM) was used to analyze the surface morphology of different fiber mats and to measure the diameters of individual fibers. The electrospinning process produced defect-free fibers with random orientation, which is crucial for consistent fiber dissolution and controlled bacteriophage release. The random orientation also contributes to the mechanical strength of the fibers, allowing the packaging to resist tensile forces from any direction during handling. The average fiber

diameters ranged from 100 to 300 nm across all specimens, with a uniform size distribution, indicating consistent and reliable fabrication. Notably, PCL fibers exhibited slightly larger diameters compared to PVA fibers; however, blending PCL with PVA led to a reduction in fiber size. The incorporation of nanocellulose into the PVA-PCL nanofibers resulted in a slightly rougher surface morphology, suggesting the successful

integration of nanocellulose within the nanofiber matrix. Notably, all fibers displayed uniformity without beads or anomalies. Fig 7.f demonstrates effective bacteriophage immobilization within the fiber matrix. Analyzing the surface structure of the fibers via electron microscopy was crucial, as the fiber architecture impacts the efficiency of bacteriophage preservation following the electrospinning process (Korehei & Kadla, 2013).

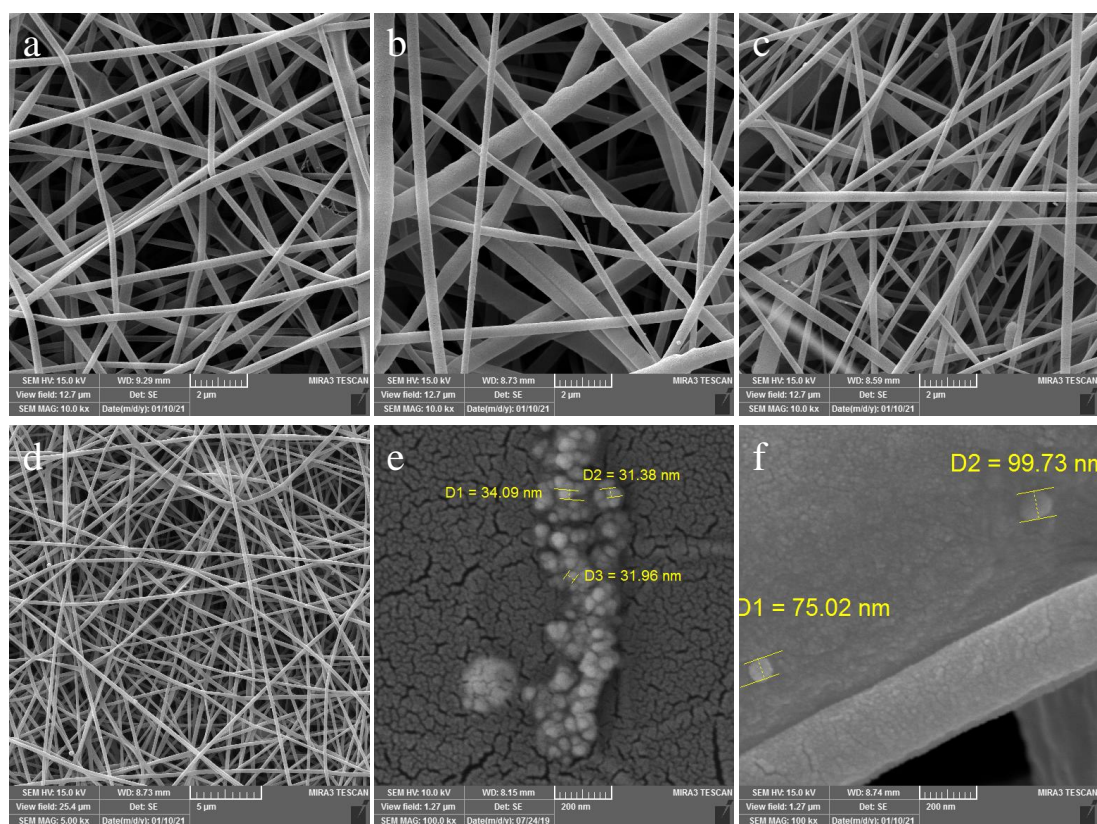


Fig 7. SEM micrographs of the surfaces of (a) Poly vinyl alcohol (PVA) nanofiber, (b) Polycaprolactone (PCL) nanofiber, (c) PVA-PCL nanofiber, (d) PVA-PCL nanofiber containing nanocellulose (NC), (e) bacteriophages, (f) and bacteriophages containing PVA-PCL-NC nanofiber.

3.7. Antibacterial activity

3.7.1. Observation of the Antimicrobial Effect of Phage and Morphology and Classification of Bacteriophages

The specific lytic phage targeting *Escherichia coli* bacteria demonstrated a strong antimicrobial effect, forming clear plaques on an

LB agar culture medium inoculated with *E. coli* bacteria. These lysed spots on the culture medium surface were clearly visible (Fig 8.a). The phage titer in the solution was quantified using Equation 1, resulting in an estimated titer of 10^{10} PFU/mL. Following negative staining and morphological examination under an electron microscope, the isolated bacteriophages

were classified into the Siphoviridae and Podoviridae families (Fig 8.b).

Ensuring effective control and rapid identification of foodborne pathogens is essential for maintaining food safety. Active

packaging, which incorporates films and antimicrobial agents, acts as a preventive strategy to limit or reduce microbial growth on food surfaces. Bacteriophages, as natural antimicrobial agents, offer a promising solution for food applications (Wang et al., 2023).

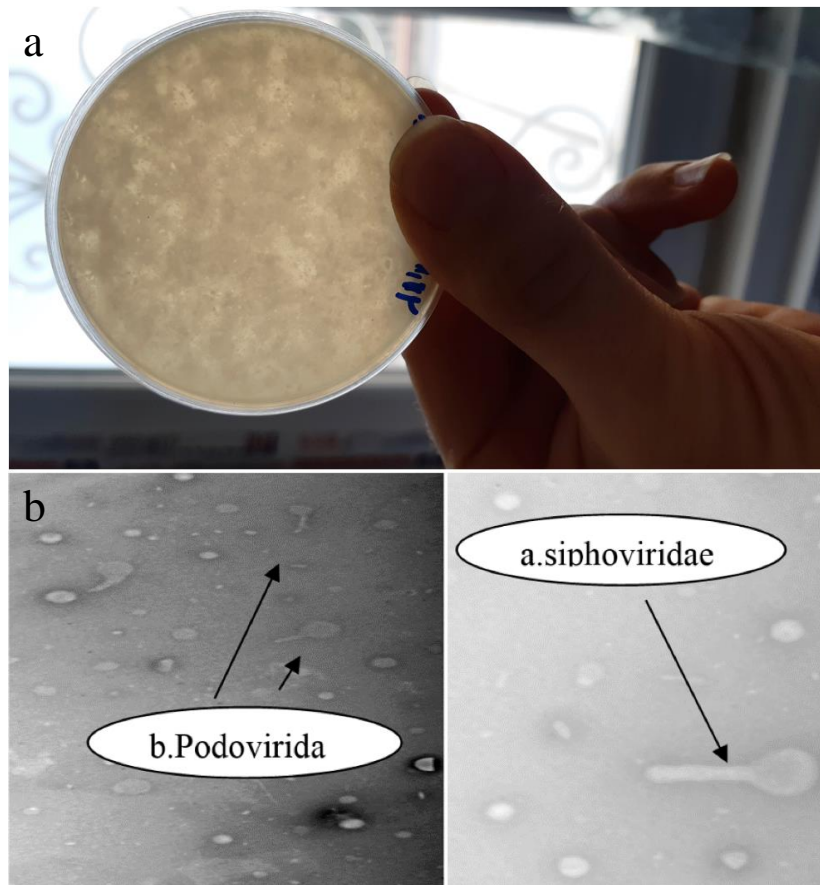


Fig 8. a. *Escherichia coli* bacteria undergoing lysis induced by bacteriophage. b. TEM microscope images of bacteriophages isolated from the coastal waters of the Caspian Sea, displayed (a. Belonging to the Siphoviridae family. b. Belonging to the Podoviridae family).

3.4. Observation of the Antimicrobial Activity of Active Electrospun Nanofibers from PVA, PCL, BNC Matrix, and Bacteriophage

The antimicrobial efficacy of electrospun nanofibers was evaluated in MHA culture medium inoculated with *Escherichia coli* at 37°C. The antimicrobial activity of immobilized bacteriophages against *E. coli* was qualitatively assessed by measuring the diameter of the

inhibition zone. Electrospun nanofibers without phages (negative control) showed no inhibition zone, while the ampicillin disk (positive control) created a 12-mm diameter zone. In contrast, electrospun nanofibers incorporating bacteriophages demonstrated a 13-mm diameter inhibition zone, indicating a specific lytic antimicrobial effect, comparable to the antibiotic (Fig 9).

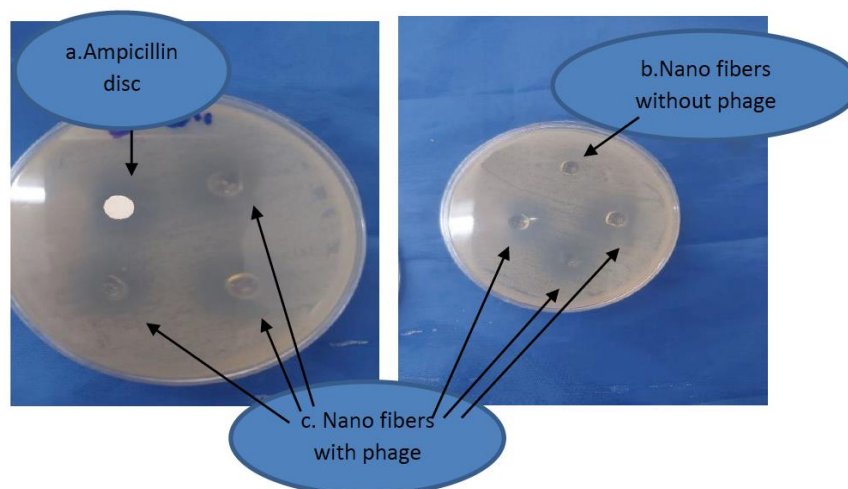


Fig 9. Represents the qualitative determination of the antimicrobial activity of immobilized phages against *Escherichia coli* by disc diffusion method.

3.5. Evaluation of Antimicrobial Ability of Phages Encapsulated in Nanofibers Over Time

After storing active nanofibers (with immobilized phages) and control samples (without phages) for one month at three different temperatures (24°C, 4°C, and -20°C), their antimicrobial effectiveness was evaluated. In a suspension containing 10^3 CFU/mL *Escherichia coli* bacteria, the remaining bacterial population was quantified at 5-day intervals over the course of 30 days. The control samples without phages exhibited no antimicrobial effect. Active nanofibers containing bacteriophages gradually lost antibacterial activity after one month at 24°C. However, nanofibers stored at 4°C and -20°C maintained their ability to lyse and destroy the target bacteria even after one month of storage (Fig 10).

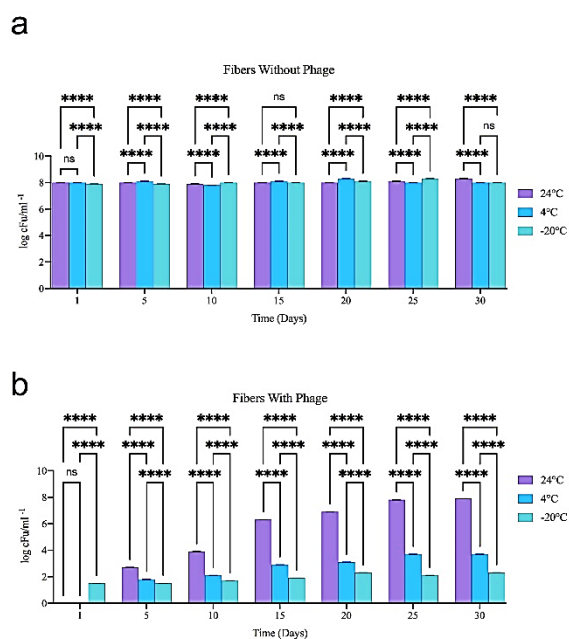


Fig 10. Results depicting the antimicrobial activity of electro-spun fibers a) without phage, b) with phage, over one month after storage at 24°C, 4°C, and -20°C. Data denote mean \pm SD (n = 3); The value of P < 0.05 was considered statistically significant. ns = not significant (p > 0.05); *p \leq 0.05; **p \leq 0.01; ***p \leq 0.001; ****p \leq 0.0001., against multiple comparisons.



Bacteriophages exhibit characteristics akin to living organisms, including reproduction, genetic information, mutation, and evolution (Abedon, 2023). Combining bacteriophages with nanofibers facilitates the maintenance of their viability over extended periods. Nanofibers, acting as carriers for biological materials like bacteriophages, offer a promising avenue for combating bacterial infections (Kielholz et al., 2023). Despite the challenges posed by the electrospinning technique, especially the high voltage involved, research suggests that encapsulating living cells, bacteriophages, and biological compounds within nanofibers is both feasible and advantageous.

Electrospinning, a specialized method for producing nanofibers, creates a network of polymeric nanofibers resembling a thin plastic layer. Incorporating biological products, sensitive to environmental factors, into nanofibers using electrospinning might seem challenging. However, various studies, including those encapsulating living cells, bacteriophages, and nucleic acids, demonstrate the feasibility and benefits of this approach. The rationale is to shield these biological entities from environmental factors, improve their quality and stability, and create flexible and practical materials through immobilization, drying, and freezing. Notably, nanofibers serve as effective carriers for medical treatments, offering protection, scaffolding for growth, and enhanced transfer capabilities. Natural and synthetic polymers, such as PEO, PVA, cellulose, and chitosan, have been employed to produce nanofibers encapsulating various biological agents, each offering specific advantages.

Previous studies have successfully demonstrated the antimicrobial effects of bacteriophages encapsulated in electrospun nanofibers. For instance, bacteriophage VB-Pae-Kakheti 25 capsid immobilized in electrospun PCL

nanofibers exhibited antibacterial effects against *Pseudomonas aeruginosa*, a pathogen causing skin infections (Nogueira et al., 2017).

Similarly, bacteriophages T4, T7, and λ maintained their viability when enclosed in PVA nanofibers for over three months at sub-zero temperatures (Salalha et al., 2006).

Furthermore, specific lytic phages isolated from wastewater and sewage samples demonstrated antimicrobial effects against *Escherichia coli*, forming plaques on culture mediums (Dallal et al., 2016).

4. Conclusions

In conclusion, the development of active packaging incorporating bacteriophages presents a promising strategy for enhancing food safety by mitigating microbial contamination. This study investigated the fabrication, characterization, and functional properties of electrospun nanofiber mats containing bacteriophages for antimicrobial applications. The electrospinning process yielded defect-free fibers with random orientation, essential for consistent fiber dissolution and bacteriophage release. The resulting fiber mats exhibited consistent fiber diameters and morphology, with successful immobilization of bacteriophages within the matrix confirmed through electron microscopy. Chemical analysis confirmed the retention of polymer properties in the electrospun fibers, ensuring the integrity of the bioactive cargo. Mechanical testing demonstrated the isotropic nature of the fiber mats, with blends of PVA, PCL, and nanocellulose offering a balance between strength and flexibility. Further characterization revealed the hygroscopic nature of PVA-based fibers, while PCL exhibited hydrophobic behavior. The blending PVA and PCL modulated the surface properties, influencing moisture absorption and contact angle. However, the incorporation of nanocellulose minimally affected surface wettability. The study

underscores the potential of electrospun nanofiber mats as effective carriers for bacteriophages, offering sustained release and antimicrobial activity. Future research should focus on optimizing fabrication parameters and evaluating the long-term stability and efficacy of bacteriophages within the nanofiber matrices. Overall, the findings contribute to the advancement of active packaging technologies aimed at enhancing food safety and reducing the risk of foodborne illnesses through targeted antimicrobial interventions.

Acknowledgements

The support of colleagues at the research center of Tabriz University of Medical Sciences Faculty of Nutrition and Health is acknowledged.

Founding source

This study was part of Malahat Safavi Ph.D. thesis and was financially supported by the Department of Food Industry Science and Technology, Faculty of Agriculture, University of Tabriz.

Data availability statement

The data that support the findings of this study are available from the corresponding author upon reasonable request.

Conflict of interest

The authors have declared no conflict of interest.

References

- [1] Abedon, S. T. (2023). Bacteriophage Adsorption: Likelihood of Virion Encounter with Bacteria and Other Factors Affecting Rates [Review]. *Antibiotics*, 12(4), Article 723.
<https://doi.org/10.3390/antibiotics12040723>
- [2] Ahn, K., Park, K., Sadeghi, K., & Seo, J. (2024). New Surface Modification of Hydrophilic Polyvinyl Alcohol via Predrying and Electrospinning of

Hydrophobic Polycaprolactone Nanofibers [Article]. *Foods*, 13(9), Article 1385.

<https://doi.org/10.3390/foods13091385>

- [3] Anany, H., Chen, W., Pelton, R., & Griffiths, M. W. (2011). Biocontrol of *Listeria monocytogenes* and *Escherichia coli* O157:H7 in meat by using phages immobilized on modified cellulose membranes [Article]. *Applied and environmental microbiology*, 77(18), 6379-6387.

<https://doi.org/10.1128/AEM.05493-11>

- [4] Azari, A., Golchin, A., Maymand, M. M., Mansouri, F., & Ardeshtyrlajimi, A. (2022). Electrospun Polycaprolactone Nanofibers: Current Research and Applications in Biomedical Application [Review]. *Advanced Pharmaceutical Bulletin*, 12(4), 658-672.

<https://doi.org/10.34172/apb.2022.070>

- [5] Bhardwaj, N., & Kundu, S. C. (2010). Electrospinning: A fascinating fiber fabrication technique. *Biotechnology advances*, 28(3), 325-347.

- [6] Chen, Z., Wei, B., Mo, X., Lim, C. T., Ramakrishna, S., & Cui, F. (2009). Mechanical properties of electrospun collagen-chitosan complex single fibers and membrane [Article]. *Materials Science and Engineering C*, 29(8), 2428-2435.
<https://doi.org/10.1016/j.msec.2009.07.006>

- [7] Cho, M.-J., & Park, B.-D. (2011). Tensile and thermal properties of nanocellulose-reinforced poly (vinyl alcohol) nanocomposites. *Journal of Industrial and Engineering Chemistry*, 17(1), 36-40.

- [8] Dallal, M. M. S., Imeni, S. M., Nikkhahi, F., Rajabi, Z., & Salas, S. P. (2016). Isolation of *E. Coli* bacteriophage from raw sewage and comparing its antibacterial effect with ceftriaxone antibiotic. *Int J Adv Biotechnol Res*, 7(3), 385-391.

- [9] Doyle, M. P., & Schoeni, J. L. (1987). Isolation of *Escherichia coli* O157:H7 from retail fresh meats and poultry [Article]. *Applied and environmental microbiology*, 53(10), 2394-2396.

<https://doi.org/10.1128/aem.53.10.2394-2396.1987>

- [10] Dufresne, A. (2013). Nanocellulose: A new ageless bionanomaterial [Review]. *Materials Today*, 16(6), 220-227.

<https://doi.org/10.1016/j.mattod.2013.06.004>

- [11] Ejara, T. M., Balakrishnan, S., & Kim, J. C. (2021). Nanocomposites of PVA/cellulose nanocrystals: Comparative and stretch drawn

- properties [Article]. *SPE Polymers*, 2(4), 288-296. <https://doi.org/10.1002/pls2.10057>
- [12] Ghosh, C., Sarkar, P., Issa, R., & Haldar, J. (2019). Alternatives to Conventional Antibiotics in the Era of Antimicrobial Resistance [Review]. *Trends in Microbiology*, 27(4), 323-338. <https://doi.org/10.1016/j.tim.2018.12.010>
- [13] Goddard, J. M., & Hotchkiss, J. H. (2007). Polymer surface modification for the attachment of bioactive compounds [Review]. *Progress in Polymer Science (Oxford)*, 32(7), 698-725. <https://doi.org/10.1016/j.progpolymsci.2007.04.002>
- [14] Hagens, S., & Loessner, M. J. (2010). Bacteriophage for biocontrol of foodborne pathogens: Calculations and considerations [Review]. *Current Pharmaceutical Biotechnology*, 11(1), 58-68. <https://doi.org/10.2174/138920110790725429>
- [15] Huang, D., Hu, Z.-D., Ding, Y., Zhen, Z.-C., Lu, B., Ji, J.-H., & Wang, G.-X. (2019). Seawater degradable PVA/PCL blends with water-soluble polyvinyl alcohol as degradation accelerator. *Polymer Degradation and Stability*, 163, 195-205.
- [16] Jamróz, E., Kulawik, P., & Kopel, P. (2019). The effect of nanofillers on the functional properties of biopolymer-based films: A review [Review]. *Polymers*, 11(4), Article 675. <https://doi.org/10.3390/polym11040675>
- [17] Ji, X., Guo, J., Guan, F., Liu, Y., Yang, Q., Zhang, X., & Xu, Y. (2021). Preparation of electrospun polyvinyl alcohol/nanocellulose composite film and evaluation of its biomedical performance [Article]. *Gels*, 7(4), Article 223. <https://doi.org/10.3390/gels7040223>
- [18] Jiang, Z., Nguyen, B. T. D., Seo, J., Hong, C., Kim, D., Ryu, S., Lee, S., Lee, G., Cho, Y. H., Kim, J. F., & Lee, K. (2023). Superhydrophobic polydimethylsiloxane dip-coated polycaprolactone electrospun membrane for extracorporeal membrane oxygenation [Article]. *Journal of Membrane Science*, 679, Article 121715. <https://doi.org/10.1016/j.memsci.2023.121715>
- [19] Khoo, R., Ismail, H., & Chow, W. (2016). Thermal and morphological properties of poly (lactic acid)/nanocellulose nanocomposites. *Procedia Chemistry*, 19, 788-794.
- [20] Kielholz, T., Rohde, F., Jung, N., & Windbergs, M. (2023). Bacteriophage-loaded functional nanofibers for treatment of *P. aeruginosa* and *S. aureus* wound infections [Article]. *Scientific Reports*, 13(1), Article 8330. <https://doi.org/10.1038/s41598-023-35364-5>
- [21] Korehei, R., & Kadla, J. (2013). Incorporation of T4 bacteriophage in electrospun fibres [Article]. *Journal of Applied Microbiology*, 114(5), 1425-1434. <https://doi.org/10.1111/jam.12158>
- [22] Li, Y., Han, C., Yu, Y., & Xiao, L. (2020). Effect of loadings of nanocellulose on the significantly improved crystallization and mechanical properties of biodegradable poly (ϵ -caprolactone). *International journal of biological macromolecules*, 147, 34-45.
- [23] Liu, B., Wu, S., Song, Q., Zhang, X., & Xie, L. (2006). Two novel bacteriophages of thermophilic bacteria isolated from deep-sea hydrothermal fields [Article]. *Current Microbiology*, 53(2), 163-166. <https://doi.org/10.1007/s00284-005-0509-9>
- [24] Mahoutforoush, A., Asadollahi, L., Hamishehkar, H., Abbaspour-Ravasjani, S., Solouk, A., & Nazarpak, M. H. (2023). Targeted Delivery of Pennyroyal via Methotrexate Functionalized PEGylated Nanostructured Lipid Carriers into Breast Cancer Cells; A Multiple Pathways Apoptosis Activator [Article]. *Advanced Pharmaceutical Bulletin*, 13(4), 747-760. <https://doi.org/10.34172/apb.2023.077>
- [25] Meng, L., Ding, S., Li, W., Liu, D., & Liu, E. (2024). Preparation and property analysis of cellulose reinforced carbon nanocomposite hydrogels [Article]. *New Journal of Chemistry*, 48(27), 12138-12145. <https://doi.org/10.1039/d4nj01692k>
- [26] Meng, L., Li, J., Fan, X., Wang, Y., Xiao, Z., Wang, H., Liang, D., & Xie, Y. (2023). Improved mechanical and antibacterial properties of polyvinyl alcohol composite films using quaternized cellulose nanocrystals as nanofillers [Article]. *Composites Science and Technology*, 232, Article 109885. <https://doi.org/10.1016/j.compscitech.2022.109885>
- [27] Meshkani, M., Mortazavi, A., & Pourfallah, Z. (2013). Antimicrobial and physical properties of a chickpea protein isolate-based film containing essential oil of thyme using response surface methodology. *Iranian Journal of Nutrition Sciences & Food Technology*, 8(1), 93-104.

- [28] Moon, R. J., Martini, A., Naim, J., Simonsen, J., & Youngblood, J. (2011). Cellulose nanomaterials review: Structure, properties and nanocomposites [Article]. *Chemical Society Reviews*, 40(7), 3941-3994.
<https://doi.org/10.1039/c0cs00108b>
- [29] Nazari, M., Majdi, H., Milani, M., Abbaspour-Ravasjani, S., Hamishehkar, H., & Lim, L. T. (2019). Cinnamon nanophytosomes embedded electrospun nanofiber: Its effects on microbial quality and shelf-life of shrimp as a novel packaging [Article]. *Food Packaging and Shelf Life*, 21, Article 100349. <https://doi.org/10.1016/j.foodhyd.2019.100349>
- [30] Nogueira, F., Karumidze, N., Kusradze, I., Goderdzishvili, M., Teixeira, P., & Gouveia, I. C. (2017). Immobilization of bacteriophage in wound-dressing nanostructure [Article]. *Nanomedicine: Nanotechnology, Biology, and Medicine*, 13(8), 2475-2484.
<https://doi.org/10.1016/j.nano.2017.08.008>
- [31] Palali, S. (2019). Cellulose Nanocrystals: Potential Replacement for Food Packaging. *Science*(July), 39-73.
- [32] Panchal, P., Ogunsona, E., & Mekonnen, T. (2019). Trends in advanced functional material applications of nanocellulose [Review]. *Processes*, 7(1), Article 10. <https://doi.org/10.3390/pr7010010>
- [33] Ranjbar, M., Sharifan, A., Shabani, S., & Amin Afshar, M. (2014). The Antimicrobial Effect of Garlic Extract on *Staphylococcus aureus* and *Escherichia coli* O157: H7 in Ready to Cook Chicken. *Journal of Food Technology and Nutrition*, 11(4), 57-66.
- [34] Rasheed, M. H., Kadhim, Q. S., Mohaimed, A. A., & Alsaedi, R. J. (2024). Synthesis and Evaluation Structural, Thermal and Electrical Properties for PCL/TiO₂ Nanocomposites. *Transactions on Electrical and Electronic Materials*, 1-11.
- [35] Ribeiro, A. S., Costa, S. M., Ferreira, D. P., Calhelha, R. C., Barros, L., Stojković, D., Soković, M., Ferreira, I. C. F. R., & Figueiro, R. (2021). Chitosan/nanocellulose electrospun fibers with enhanced antibacterial and antifungal activity for wound dressing applications [Article]. *Reactive and Functional Polymers*, 159, Article 104808.
<https://doi.org/10.1016/j.reactfunctpolym.2020.104808>
- [36] Salalha, W., Kuhn, J., Dror, Y., & Zussman, E. (2006). Encapsulation of bacteria and viruses in electrospun nanofibres [Article]. *Nanotechnology*, 17(18), 4675-4681, Article 025.
<https://doi.org/10.1088/0957-4484/17/18/025>
- [37] Salari, M., Sowti Khiabani, M., Rezaei Mokarram, R., Ghanbarzadeh, B., & Samadi Kafil, H. (2018). Development and evaluation of chitosan based active nanocomposite films containing bacterial cellulose nanocrystals and silver nanoparticles [Article]. *Food Hydrocolloids*, 84, 414-423.
<https://doi.org/10.1016/j.foodhyd.2018.05.037>
- [38] Shen, H. Y., Liu, Z. H., Hong, J. S., Wu, M. S., Shiue, S. J., & Lin, H. Y. (2021). Controlled-release of free bacteriophage nanoparticles from 3D-plotted hydrogel fibrous structure as potential antibacterial wound dressing [Article]. *Journal of Controlled Release*, 331, 154-163.
<https://doi.org/10.1016/j.jconrel.2021.01.024>
- [39] Singhaboot, P., Kraisuan, W., Chatkumpjunjaleam, T., Kroeksakul, P., & Chongkolnee, B. (2023). Development and Characterization of Polyvinyl Alcohol/Bacterial Cellulose Composite for Environmentally Friendly Film [Article]. *Journal of Ecological Engineering*, 24(6), 226-238.
<https://doi.org/10.12911/22998993/162954>
- [40] Tolba, M., Minikh, O., Brovko, L. Y., Evoy, S., & Griffiths, M. W. (2010). Oriented immobilization of bacteriophages for biosensor applications [Article]. *Applied and environmental microbiology*, 76(2), 528-535.
<https://doi.org/10.1128/AEM.02294-09>
- [41] Topuz, F., Kilic, M. E., Durgun, E., & Szekely, G. (2021). Fast-dissolving antibacterial nanofibers of cyclodextrin/antibiotic inclusion complexes for oral drug delivery [Article]. *Journal of Colloid and Interface Science*, 585, 184-194.
<https://doi.org/10.1016/j.jcis.2020.11.072>
- [42] Vonasek, E., Le, P., & Nitin, N. (2014). Encapsulation of bacteriophages in whey protein films for extended storage and release [Article]. *Food Hydrocolloids*, 37, 7-13.
<https://doi.org/10.1016/j.foodhyd.2013.09.017>
- [43] Wang, B., Wang, H., Lu, X., Zheng, X., & Yang, Z. (2023). Recent Advances in



Electrochemical Biosensors for the Detection of Foodborne Pathogens: Current Perspective and Challenges [Review]. *Foods*, 12(14), Article 2795. <https://doi.org/10.3390/foods12142795>

[44] Xiao, M., Chery, J., & Frey, M. W. (2018). Functionalization of Electrospun Poly(vinyl alcohol) (PVA) Nanofiber Membranes for Selective Chemical Capture [Article]. *ACS Applied Nano Materials*, 1(2), 722-729.

<https://doi.org/10.1021/acsanm.7b00180>

[45] Zhao, Y., Sun, H., Yang, B., & Weng, Y. (2020). Hemicellulose-based film: Potential green films for food packaging [Review]. *Polymers*, 12(8), Article 1775. <https://doi.org/10.3390/polym12081775>

[46] Zheng, T., Clemons, C. M., & Pilla, S. (2021). Grafting PEG on cellulose nanocrystals via polydopamine chemistry and the effects of PEG graft length on the mechanical performance of composite film [Article]. *Carbohydrate Polymers*, 271, Article 118405.

<https://doi.org/10.1016/j.carbpol.2021.118405>

[47] Zhou, C., Chu, R., Wu, R., & Wu, Q. (2011). Electrospun polyethylene oxide/cellulose nanocrystal composite nanofibrous mats with homogeneous and heterogeneous microstructures [Article]. *Biomacromolecules*, 12(7), 2617-2625. <https://doi.org/10.1021/bm200401p>

[48] Zhou, H., Green, T. B., & Joo, Y. L. (2006). The thermal effects on electrospinning of polylactic acid melts. *Polymer*, 47(21), 7497-7505.

[49] Zidan, H. M., Abdelrazek, E. M., Abdelghany, A. M., & Tarabiah, A. E. (2019). Characterization and some physical studies of PVA/PVP filled with MWCNTs [Article]. *Journal of Materials Research and Technology*, 8(1), 904-913.

<https://doi.org/10.1016/j.jmrt.2018.04.023>

مقاله پژوهشی

توسعه و ویژگی‌های نانو بیوکامپوزیت هوشمند PVA/NC/PCL با استفاده از فاز *E. coli*: بررسی خواص فیزیکوشیمیایی و فعالیت ضد میکروبی

ملاحت صفوی^۱، رضا رضایی مکرّم^{۱*}، محمود صوتی خیابانی^۱، علیرضا استاد رحیمی^۲، ابولفضل برزگر^۳

۱. گروه علوم و مهندسی صنایع غذایی، دانشکده کشاورزی، دانشگاه تبریز.

۲. مرکز تحقیقات تغذیه، دانشکده تغذیه و علوم غذایی، دانشگاه علوم پزشکی تبریز.

۳. مرکز تحقیقات علوم پایه، دانشگاه تبریز.

چکیده:

بسته‌بندی مواد غذایی نقش مهمی در حفظ تازگی و کیفیت مواد غذایی و جلوگیری از فساد میکروبی ایفا می‌کند. پیشرفت‌ها در این حوزه به توسعه سیستم‌های بسته‌بندی هوشمند و فعال با بهره‌گیری از فناوری نانو منجر شده است. در میان این نوآوری‌ها، الکترورسی برای تولید نانو الیاف با نسبت سطح به حجم بالا مورد توجه قرار گرفته است که امکان بارگذاری مؤثر عوامل فعال را فراهم می‌کند. با توجه به نگرانی‌های فزاینده درباره باکتری‌های مقاوم به آنتی‌بیوتیک، این مطالعه به بررسی استفاده از باکتریوفازها به‌عنوان یک عامل ضد میکروبی جایگزین پرداخته است. باکتریوفازهای لیتیک با هدف قرار دادن اشریشیا کلی از آب دریای خزر جداسازی شده و بر روی نانوفیبرهای الکترورسی شده ساخته شده از پلی‌وینیل الکل (PVA)، پلی‌کاپرولاکتون (PCL) و نانوسلولز باکتریایی (BNC) تثبیت شدند. تصاویر میکروسکوپ الکترونی روبشی (SEM) تثبیت موفقیت‌آمیز فازها را تأیید کرد، در حالی که میکروسکوپ الکترونی عبوری (TEM) نشان داد که این فازها به خانواده‌های Siphoviridae و Podoviridae تعلق دارند. افزودن PCL به PVA استحکام مکانیکی نانوفیبرها را افزایش داد، عیوب ساختاری را کاهش داد و مقاومت آن‌ها را در برابر آب بهبود بخشید؛ همچنین افزودن BNC ساختار نانوفیبرها را تقویت کرد و خواص ماترسی آن‌ها را ارتقا داد. آزمایش‌های ضد میکروبی با استفاده از روش انتشار دیسک، هاله مهاری به قطر ۱۳ میلی‌متر را نشان داد که از عملکرد آنتی‌بیوتیک آمپی‌سیلین فراتر بود. نکته قابل توجه این که نانوفیبرهای عامل‌دار شده تا یک ماه کارایی ضد میکروبی خود را حفظ کردند و پایداری فازها در دماهای ۲۴ درجه سانتی‌گراد، ۴ درجه سانتی‌گراد و ۲۰- درجه سانتی‌گراد تأیید شد. این یافته‌ها نشان‌دهنده پتانسیل بالای نانوفیبرهای الکترورسی شده عامل‌دار با باکتریوفازها به‌عنوان یک راه‌حل پایدار برای مقابله با آلودگی باکتریایی در بسته‌بندی مواد غذایی است که می‌تواند ایمنی مواد غذایی را افزایش داده و عمر مفید آن‌ها را طولانی‌تر می‌کند.

کلمات کلیدی: باکتریوفازها، الکترورسی، پلی‌کاپرولاکتون، پلی‌وینیل الکل، نانوفیبر، نانوسلولز باکتریایی.